

# Development of Calpain-specific Inactivators by Screening of Positional Scanning Epoxide Libraries<sup>\*[S]</sup>

Received for publication, November 7, 2006, and in revised form, December 12, 2006. Published, JBC Papers in Press, January 11, 2007, DOI 10.1074/jbc.M610372200

Dominic Cuerrier<sup>†1</sup>, Tudor Moldoveanu<sup>‡2</sup>, Robert L. Campbell<sup>‡</sup>, Jacqueline Kelly<sup>‡</sup>, Bilge Yoruk<sup>‡</sup>, Steven H. L. Verhelst<sup>§</sup>, Doron Greenbaum<sup>§3</sup>, Matthew Bogyo<sup>§</sup>, and Peter L. Davies<sup>†1,4</sup>

From the <sup>†</sup>Department of Biochemistry and <sup>‡</sup>Protein Function Discovery Group, Queen's University, Kingston, Ontario K7L 3N6, Canada and the <sup>§</sup>Department of Pathology, Stanford University School of Medicine, Stanford, California 94305

Calpains are calcium-dependent proteases that are required for numerous intracellular processes but also play an important role in the development of pathologies such as ischemic injury and neurodegeneration. Many current small molecule calpain inhibitors also inhibit other cysteine proteases, including cathepsins, and need improved selectivity. The specificity of inhibition of several calpains and papain was profiled using synthetic positional scanning libraries of epoxide-based compounds that target the active-site cysteine. These peptidomimetic libraries probe the P4, P3, and P2 positions, display (*S,S*)- or (*R,R*)-epoxide stereochemistries, and incorporate both natural and non-natural amino acids. To facilitate library screening, an SDS-PAGE assay that measures the extent of hydrolysis of an inactive recombinant m-calpain was developed. Individual epoxide inhibitors were synthesized guided by calpain-specific preferences observed from the profiles and tested for inhibition against calpain. The most potent compounds were assayed for specificity against cathepsins B, L, and K. Several compounds demonstrated high inhibition specificity for calpains over cathepsins. The best of these inhibitors, WRH(*R,R*), irreversibly inactivates m- and  $\mu$ -calpain rapidly ( $k_2/K_i = 131,000$  and  $16,500 \text{ M}^{-1} \text{ s}^{-1}$ , respectively) but behaves exclusively as a reversible and less potent inhibitor toward the cathepsins. X-ray crystallography of the proteolytic core of rat  $\mu$ -calpain inactivated by the epoxide compounds WR  $\gamma$ -cyano- $\alpha$ -aminobutyric acid (*S,S*) and WR allylglycine (*R,R*) reveals that the stereochemistry of the

epoxide influences positioning and orientation of the P2 residue, facilitating alternate interactions within the S2 pocket. Moreover, the WR  $\gamma$ -cyano- $\alpha$ -aminobutyric acid (*S,S*)-complexed structure defines a novel hydrogen-bonding site within the S2 pocket of calpains.

Calpains form a family of calcium-dependent proteolytic enzymes found in the cytosol and at the cell and endoplasmic reticulum membranes, where they modulate signal transduction pathways by converting transient calcium influxes into a proteolytic signal. The major calpain isoforms,  $\mu$ - and m-calpains (also known as calpains 1 and 2), cleave a wide variety of proteins in the cell, including the cytoskeletal proteins  $\alpha$ -spectrin, integrin subunit  $\beta$ 3 and filamin A, the CDK5 regulator p35 (1), and the mitochondrial membrane permeability factor Bax (2), supporting their involvement in a wide variety of cellular processes ranging from cell motility (3) and cell cycling (4) to cell death by apoptosis and necrosis (5). When a cell loses its ability to control calcium levels following an ischemic episode or acute neural/cerebral injury, calpains are constitutively activated and contribute to furthering cell damage by degrading nontarget proteins such as other cytoskeletal components, resulting in apoptosis or necrosis and irreversible tissue damage (6). In a similar manner but on a different time scale, calpain overactivation also contributes to the development of cataracts and Alzheimer disease. Other calpain isoforms are linked to the development of specific pathologies such as calpain 3 in limb girdle muscular dystrophy type IIA (7, 8), calpain 10 in type II diabetes (9), and calpain 9 in gastric cancer (10). Therefore, calpains represent potential/promising drug targets for the treatment of these conditions (11–14).

The broad cleavage specificity of calpains, along with the similar specificities of other clan CA proteases, including cathepsins (15), has been a major obstacle in the development of therapeutic calpain inhibitors (16). Many calpain-inhibitory compounds that are currently in use, like calpeptin, MDL-28170, and ALLN, can cross-react with cathepsins, papain, and even, to some degree, with the proteasome (17–20). Indeed, the normal physiological roles of calpains remain poorly defined, partly because calpain-specific inhibitors are not available. Therefore, the development of calpain inhibitors with improved specificity is necessary both to further the understanding of this protease family in cell regulation and disease and as potential leads for therapeutic agents.

\* This work was supported in part by grants from the Heart and Stroke Foundation of Ontario and the Canadian Institutes of Health Research (to P. L. D.), National Technology Center for Networks and Pathways Grant U54 RR020843 from the National Institutes of Health, and National Institutes of Health Grant R01-EB005011 (to M. B.). The costs of publication of this article were defrayed in part by the payment of page charges. This article must therefore be hereby marked "advertisement" in accordance with 18 U.S.C. Section 1734 solely to indicate this fact.

The atomic coordinates and structure factors (code 2NQG and 2NQI) have been deposited in the Protein Data Bank, Research Collaboratory for Structural Bioinformatics, Rutgers University, New Brunswick, NJ (<http://www.rcsb.org/>).

[S] The on-line version of this article (available at <http://www.jbc.org>) contains supplemental Table 1.

<sup>1</sup> Supported by the Government of Canada Natural Sciences and Engineering Research Council studentship.

<sup>2</sup> Holds a Canadian Institutes of Health Research postdoctoral fellowship. Present address: Dept. of Immunology, St. Jude Children's Research Hospital, 332 N. Lauderdale, Memphis, TN 38105.

<sup>3</sup> Present address: Dept. of Pharmacology, School of Medicine, University of Pennsylvania, Philadelphia, PA 19104-6160.

<sup>4</sup> Holds a Canada Research Chair in Protein Engineering. To whom correspondence should be addressed: Dept. of Biochemistry, Botterell Hall, Queen's University, Kingston, Ontario K7L 3N6, Canada. Tel.: 613-533-2984; Fax: 613-533-2497; E-mail: [daviesp@post.queensu.ca](mailto:daviesp@post.queensu.ca).

Mini-calpains, recombinant fragments of the full-length enzyme composed exclusively of the proteolytic domains I and II, can be used as surrogates to study the proteolytic activity of calpains (21–24). These isolated proteolytic cores offer advantages over their native enzyme counterparts because they are not subject to autolysis, subunit dissociation, and aggregation. Perhaps most importantly, mini-calpains can be crystallized in the presence of  $\text{Ca}^{2+}$  with inhibitors bound at the active site, which has permitted a structure-guided approach to studying active-site-directed inhibitors of calpains (25–27).

Inhibitors containing an epoxysuccinyl electrophile as a warhead constitute a class of irreversible inactivators specific to clan CA cysteine proteases. The first naturally occurring inhibitor of this type, E-64,<sup>5</sup> isolated from *Aspergillus japonicus*, is a commonly used broad range inhibitor of these proteases (28). Mechanistically, epoxide inhibitors inactivate their target enzyme by irreversibly alkylating the nucleophilic active-site cysteine, with a peptidyl moiety serving to position the epoxide group close to the cysteine (29, 30). Synthetic analogs of E-64 consisting of an epoxide electrophile attached to a peptidyl determinant designed to increase selectivity for particular proteases have successfully resulted in highly specific inhibitors of cathepsin B (31, 32) and cathepsin L (33) and also have use as specificity profiling tools (34). Related aza-peptide epoxides are highly selective inhibitors of caspases and other clan CD proteases (35).

Combinatorial chemistry allows large numbers of compounds that systematically vary at key positions to be synthesized in parallel and in a relatively short period of time. Peptidyl compounds, with basic amide chemistries, lend themselves well to such types of synthesis. Therefore, libraries of peptidyl compounds can be made with a variety of both natural and non-natural amino acids in the recognition region using combinatorial peptide-based solid-phase synthesis.

We have applied such a library of positional scanning epoxide-based compounds in conjunction with a medium-throughput SDS-PAGE-based screening assay to profile m-calpain, the mini-calpains  $\mu\text{I-II}$  and  $\text{mI-II}$  engineered with the stabilizing mutation G203A, and the related cysteine protease papain. These preference profiles demonstrate the differences in the specificity between the proteases, including some differences in the active-site specificity between mini and full-length calpains. The observed calpain-oriented preferences were applied to design potent inhibitors of calpain that demonstrate a high degree of specificity relative to members of the cathepsin family. The most calpain-specific compound, WRH(R,R), was demonstrated to exclusively inactivate calpain irreversibly, supporting the usefulness of positional scanning libraries in the design of inhibitors and leads for activity-based probes.

## EXPERIMENTAL PROCEDURES

**Materials**—The proteases m-calpain (active and C105S inactive mutant),  $\mu\text{I-II}$ , and  $\text{mI-II}$  G203A from rat were recombi-

nantly expressed in *Escherichia coli* and purified as described previously (21, 24, 36, 37). Papain (purified from *Carica papaya*) was obtained from Fluka (Buchs, Switzerland). Cathepsin B (human liver), cathepsin L (human recombinant), and  $\mu$ -calpain (porcine erythrocyte) were obtained from Calbiochem. Cathepsin K (human) was a gift from Dr. Robert Menard. The cathepsin substrate Z-FR-AMC was obtained from Axxora (San Diego, CA). The calpain substrate (EDANS)-EPLFAERK-(DABCYL) was synthesized in the Peptide Synthesis Laboratory of the Protein Function Discovery Facility at Queen's University (Kingston, Ontario, Canada) and at the Alberta Peptide Institute (Edmonton, Alberta, Canada). All other reagents were obtained from common sources. The triple-wide gel electrophoresis apparatus is from C.B.S. Scientific (Solana Beach, CA). The positional scanning epoxide libraries were synthesized as described elsewhere (29) and used from 50 mM stocks in  $\text{Me}_2\text{SO}$ . The structures and names of the non-natural amino acids used in the P2 position are given in the supplemental Table 1.

**Screening of the Positional Scanning Libraries, Calpains**—A solution containing 1 mg/ml inactive m-calpain C105S (m-calpain with an inactivating C105S mutation) was prepared in calpain reducing buffer (50 mM HEPES-NaOH (pH 7.8) and 10 mM DTT), along with either 0.18 mg/ml  $\mu\text{I-II}$  or 0.35 mg/ml  $\text{mI-II}$  G203A or 50  $\mu\text{g/ml}$  m-calpain (for *trans* autolysis). For *cis* autolysis of m-calpain, the solution contained solely 1 mg/ml active m-calpain in the reducing buffer. Digestion was initiated by addition of an equal volume of calpain reducing buffer containing either 0.5–2 mM crude inhibitor pools and 100 mM  $\text{CaCl}_2$  ( $\mu\text{I-II}$  or  $\text{mI-II}$  G203A) or 50–200  $\mu\text{M}$  crude inhibitor pools and 2 mM  $\text{CaCl}_2$  (m-calpain). The reactions were allowed to proceed at 35 °C for 30 min (m-calpain), 60 min ( $\mu\text{I-II}$ ), or 120 min ( $\text{mI-II}$  G203A) prior to being quenched by addition of 3 $\times$  SDS-PAGE sample buffer (200 mM Tris-HCl (pH 6.8), 6% (w/v) SDS, 30% glycerol, 0.03% (w/v) bromphenol blue).

**Papain**—A solution containing 1 mg/ml of inactive m-calpain C105S and 20–160  $\mu\text{M}$  crude inhibitor pool was prepared in papain reducing buffer (50 mM HEPES-NaOH (pH 6.8) and 10 mM DTT). Digestion was initiated by the addition of an equal volume of papain reducing buffer containing 10  $\mu\text{g/ml}$  papain and 10 mM  $\text{CaCl}_2$ . The reactions were allowed to proceed at room temperature for 30 min prior to being quenched by addition of 3 $\times$  SDS-PAGE sample buffer containing 100  $\mu\text{M}$  E-64. For all calpain and papain digests, the final reaction contained <5%  $\text{Me}_2\text{SO}$ . The digests were then analyzed by SDS-PAGE using triple-wide 12% polyacrylamide gels with a 65-well comb that can accommodate 5–10  $\mu\text{l}$  of each digest sample per well. The 80-kDa subunit of m-calpain was quantitated densitometrically using the free open source software ImageJ (<http://rsb.info.nih.gov/ij/>). The background intensity corresponding to the signal immediately above the 80-kDa band was subtracted from every lane.

**Synthesis of the Epoxide Compounds**—Single epoxide compounds were made on a Rink Amide solid support following similar protocols as described previously (38). In brief, peptides were elongated making use of 20% piperidine in dimethylformamide to remove Fmoc-protecting groups and a combination of 1,3-diisopropylcarbodiimide (3 eq), hydroxybenzotriazole

<sup>5</sup> The abbreviations used are: E-64, L-*trans*-epoxysuccinyl-leucylamide-(4-guanido)-butane; DTT, dithiothreitol; Fmoc, N- $\alpha$ -(9-fluorenylmethyloxycarbonyl); MES, 2-(N-morpholino)ethanesulfonic acid; Z, benzyloxycarbonyl; AMC, 7-amino-4-methylcoumarin; HPLC, high pressure liquid chromatography.

## Epoxide Inhibitors of Calpains

(3 eq) to couple the desired amino acid (3 eq). After the final Fmoc deprotection, the free amino terminus was capped with the epoxide warhead using a nitrophenyl-activated epoxysuccinate synthon. The inhibitors were cleaved from the resin by trifluoroacetic acid/H<sub>2</sub>O/tri-isopropylsilane 18:1:1 and evaporated under reduced pressure prior to HPLC purification.

**Specificity Determination of the WRX Epoxides by a Fluorometric End Point Assay**—The fluorometric assays were performed in triplicate in 96-well plates in a final volume of 100  $\mu$ L, with concentrations of inhibitor ranging from 32 nM to 320  $\mu$ M. The end point fluorescence intensity in each well was measured in a SpectraMax Gemini fluorescence plate reader (Molecular Devices, Sunnyvale, CA), and the IC<sub>50</sub> values were obtained by three-parameter sigmoidal fitting of the logarithmic concentration-inhibition curves using the data graphing software SigmaPlot (Systat Software Inc.). Calpain inhibition was assayed in 50 mM HEPES-NaOH (pH 7.7) in the presence of 5  $\mu$ M (EDANS)-EPLFAERK-(DABCYL) (23), 1 mM CaCl<sub>2</sub>, and 0.1%  $\beta$ -mercaptoethanol using 30–40 nM calpain. The reaction was initiated by the addition of inhibitor, substrate, and CaCl<sub>2</sub>, allowed to proceed at room temperature for 20 min, and then stopped by addition of EDTA to 5 mM. Fluorescence intensities were determined using 335 nm excitation and 505 nm emission wavelengths. Cathepsin inhibition was assayed in 0.1 M NaOAc-HCl (pH 5.5), 1 mM EDTA, and 0.1%  $\beta$ -mercaptoethanol in the presence of 300 pM cathepsin B, 10 pM cathepsin L, or 100 pM cathepsin K using the substrate Z-FR-AMC (20  $\mu$ M for cathepsin B, 5  $\mu$ M for cathepsin L, and 10  $\mu$ M for cathepsin K). The cathepsins were reductively activated by preincubation in assay buffer for 20–30 min prior to initiating the reaction by addition of substrate and inhibitor. The reactions were allowed to proceed at room temperature for 20 min and then stopped by addition of E-64 to 10  $\mu$ M. Fluorescence intensities were determined using 360 nm excitation and 450 nm emission wavelengths.

**Inhibition Kinetics of WRH(R,R) against Calpains and Cathepsins**—Proteolytic activity was monitored in real time using a 1.5-ml quartz cuvette and an LS50-B luminescence spectrophotometer (PerkinElmer Life Sciences). Final Me<sub>2</sub>SO concentrations were less than 1%, and the total substrate consumed during the assay was always below 5%. All reactions were performed at room temperature. To maintain pseudo-first order conditions, the inhibitor concentration was at least four times the enzyme concentration at all times. Calpain activity was assayed in 50 mM HEPES-NaOH (pH 7.7), 0.5 mM EDTA, 5 mM CaCl<sub>2</sub>, and 0.1%  $\beta$ -mercaptoethanol in the presence of 2.5  $\mu$ M (EDANS)-EPLFAERK-(DABCYL) (23) using 25 nM  $m$ - or  $\mu$ -calpain. The reaction was initiated by the simultaneous addition of a fresh mixture of calcium and the inhibitor WRH(R,R) and monitored using excitation and emission wavelengths of 335 and 500 nm, respectively. Inhibitor concentrations were assayed in the range of 0.1–4.0  $\mu$ M. To determine inactivation kinetic constants, a pseudo-first order rate constant ( $k_{\text{obs}}$ ) was first calculated from the progress curves using the Guggenheim method as described previously (39, 40). The background inactivation rate (because of calpain autolysis) was calculated in the absence of inhibitor and subtracted from the rates obtained in the presence of inhibitor. The first order inactivation rate con-

stant ( $k_2$ ) and binding constant ( $K_i$ ) were calculated by the linear regression (slope =  $K_i/k_2$ ,  $y$ -intercept =  $1/k_2$ ) of a  $1/k_{\text{obs}}$  versus  $1/[I]$  plot as shown in Fig. 6B (41). Cathepsin activity was assayed in 0.1 M NaOAc-HCl (pH 5.5), 1 mM EDTA, and 0.1%  $\beta$ -mercaptoethanol in the presence of 730 pM cathepsin B, 6.25 pM cathepsin L, or 136 pM cathepsin K and the substrate Z-FR-AMC (20  $\mu$ M for cathepsin B, 2  $\mu$ M for cathepsin L, and 10  $\mu$ M for cathepsin K). Product formation was monitored using excitation and emission wavelengths of 360 and 440 nm, respectively. The reaction was initiated by the addition of reductively pre-activated enzyme and the activity allowed to stabilize prior to addition of an aliquot of WRH(R,R). Inhibitor concentrations were assayed in the range of 4.0–50  $\mu$ M (cathepsin B and K) or 1.0–20  $\mu$ M (cathepsin L). The apparent inhibition constant ( $K_{\text{app}}$ ) was calculated as the reciprocal of the slope of a  $(V_0/V_i) - 1$  versus  $[I]$  plot, where  $V_0$  and  $V_i$  are the uninhibited and inhibited steady-state rates, respectively, as shown in Fig. 6D. This apparent rate constant was corrected for substrate competition to yield the inhibition constant ( $K_i$ ) using the substrate concentration ( $[S]$ ), Michaelis-Menten constant ( $K_m$ ), and the following equation:  $K_i = K_{\text{app}}/(1 + [S]/K_m)$ . The  $K_m$  values used were 150  $\mu$ M for cathepsin B (42), 9.1  $\mu$ M for cathepsin K (43), and 2.4  $\mu$ M for cathepsin L (44).

**Crystallographic Determination of the  $\mu$ I-II-Epoxide Complex Structures**—HPLC-purified inhibitors were dissolved in Me<sub>2</sub>SO to a concentration of 50 mM. To form the enzyme-inhibitor complexes, 26  $\mu$ L of a working stock solution of 25 mg/ml  $\mu$ I-II in 10 mM HEPES-NaOH (pH 7.7) and 10 mM DTT was added to 26  $\mu$ L of a fresh complexing solution containing 4% Me<sub>2</sub>SO, 10 mM HEPES-NaOH (pH 7.7), 1 M NaCl, 2 mM CaCl<sub>2</sub>, and 2 mM inhibitor. The reaction was allowed to incubate at room temperature for 1 h prior to addition to the crystallization drop. Crystals of the complex were obtained using the hanging drop vapor diffusion method by mixing the above solution with an equal volume of precipitant solution using conditions expanding around 1.1–1.7 M NaCl, 10 mM CaCl<sub>2</sub>, and 0.1 M MES (pH 5.5–6.25). The crystals obtained were cryo-protected prior to data collection by soaking in a solution of the mother liquor containing 20% glycerol. Data were collected on a Rigaku RU-200 rotating anode x-ray generator (50 kV, 100 mA), with an Osmic mirror system and a 300-mm image plate detector (MAR Research). The crystals were maintained at 100 K during data collection by a cryo-cooling system (Oxford Cryosystems). Data processing and manipulation were performed using the programs Mosflm (45) and Scala of the CCP4 program suite (46). The inhibitor-complexed structures were determined by molecular replacement using MOLREP (47) with the polypeptide moiety of the  $\mu$ I-II-SNJ-1945 complex (chain A of Protein Data Bank code 2G8J) as the input model. The refinement of the model was done using REFMAC5 (48), whereas XtalView/XFit (49) was used for model building. The Dundee PRODRG2 server (50) was used to generate the molecular topology description of the ligand. All structure diagrams were generated in PyMOL (51).

**Structure Coordinates**—Coordinates for the WR18(S,S)- and WR13(R,R)- inactivated structures have been deposited with the RCSB protein Data Bank under the accession codes 2NQG and 2NQI, respectively. The P2 positions designated by 18 and

13 refer to  $\gamma$ -cyano- $\alpha$ -aminobutyric acid and allylglycine, respectively.

## RESULTS

**Specificity Profiling Using Positional Scanning Libraries**—The combinatorial epoxide libraries used here profile cysteine proteases based on their amino acid preferences at positions P2, P3, and P4 of the peptide recognition region. These libraries were previously synthesized and successfully used for profiling cathepsins (34), to generate a cathepsin B-specific inhibitor (52) and also to find a falcipain 1-specific inhibitor in *P. falciparum* (53). In brief, each pool within a library contains a fixed amino acid (1 of 19 natural amino acids: no Cys, no Met, plus norleucine) at P2, P3, or P4 and a mixture of amino acids at the other positions (Fig. 1). The P2-scanning library is expanded to also incorporate 41 non-natural amino acids into the selection at this fixed position (supplemental Table 1). Additionally, the P2-scanning libraries (both natural and non-natural) exhibit either an (*R,R*)- or (*S,S*)-epoxide stereochemistry. Therefore, a total of 158 different pools, 120 of which form the P2-scanning library, were used in the screening. The larger size of the P2-scanning library is intended to reflect the importance of this position in generating specificity for clan CA proteases.

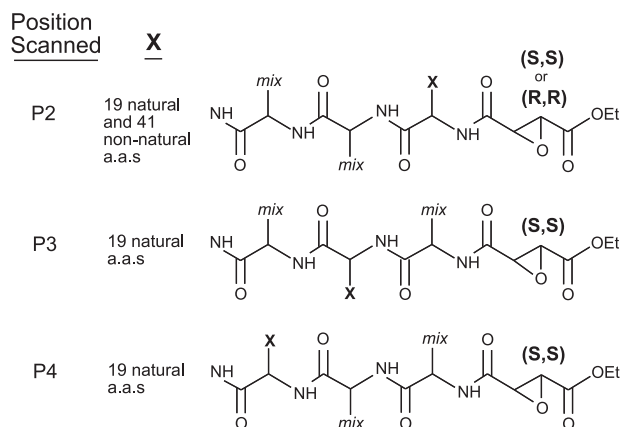


**FIGURE 1. Structural representation of the mixture-based positional scanning libraries of epoxysuccinyl compounds used to profile calpain and papain specificity.** Each pool within a library contains a fixed residue ( $\times$ ) at a position specific to the series (position scanned) and an equimolar mixture of all the natural residues (*mix*) at every other position. The P2-scanning library contains pools that have natural and non-natural amino acids (*a.a.s*) at the scanned position, as well as either (*S,S*)- or (*R,R*)-epoxide stereochemistry. The P3 and P4 libraries have (*S,S*) stereochemistry and contain only natural amino acids. The set of natural amino acids (19 residues) omits cysteine and methionine but includes norleucine. The set of non-natural amino acids (42 residues) include leucine (number 42) as a control. The sum of the libraries contains 158 different pools, with a total diversity of  $>44,000$  compounds.

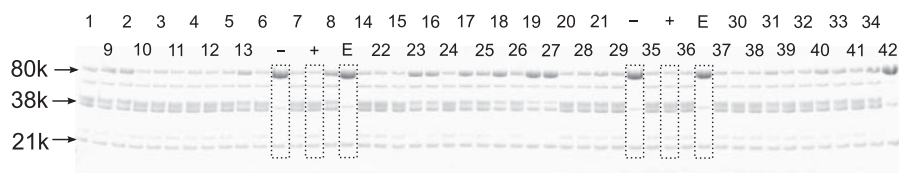


**FIGURE 2. Screening for inhibition of  $\mu$ I-II by an SDS-PAGE-based proteolytic assay.** This assay is based on the digestion of the large (80k) subunit of inactive C105S m-calpain by the test protease monitored by SDS-PAGE and Coomassie Blue staining. A representative gel of the P2-scanning non-natural (*R,R*) epoxide library screened using  $\mu$ I-II is shown. The *numbers* represent a particular non-natural amino acid fixed at the P2 position (see Supplemental Material for structures). Control lanes where the reaction was performed in the absence of inhibitor (+), absence of  $\text{Ca}^{2+}$  (-), or presence of E-64 (E) are boxed.

These libraries were screened for inhibition of native m-calpain,  $\mu$ I-II, mI-II G203A, and the distantly related papain as a control. The mini-calpains are less active than their full-length counterparts and do not perform as well in the fluorescence-based assay. Therefore, we developed an alternate method for assaying proteolytic activity in a medium-throughput manner. Previous limited proteolysis studies have shown that in the presence of  $\text{Ca}^{2+}$ , the large (80-kDa) subunit of m-calpain undergoes a significant conformational change that renders it susceptible to *in vitro* proteolysis by active calpains, trypsin and chymotrypsin (36). Because of its large size, the hydrolysis of an enzymatically inactive form of m-calpain (because of a C105S mutation) is easily monitored by SDS-PAGE. Therefore, we developed an alternate and highly sensitive method for assaying proteolytic activity in a medium-throughput manner where protease activity is monitored by the extent of digestion of the inactive m-calpain large subunit (Fig. 2). A triple-wide gel electrophoresis system allows for the simultaneous analysis of 60+ digests in a single experiment. In addition, this assay has the advantage of not being susceptible to interference from fluorophore/chromophore-containing inhibitors compared with fluorescence-based assays.

The assay conditions for each protease were optimized to obtain *almost* complete digestion of the 80-kDa band prior to quenching, allowing for a large range of inhibition to be observed (Fig. 2). Inhibition assays with m-calpain were done either in *trans* (active m-calpain digesting inactive m-calpain C105S) or in *cis* mode (active m-calpain autolysis). Both yielded similar specificity results (not shown), although the latter is preferred in practice as it shows a lower background of undigested substrate and can detect lower levels of inhibition.

The P2-scanning library screening showed a preference  $>2.0$  for residues Ile, Leu, and Val for all four proteases and demonstrated an additional preference  $>2.0$  for Phe, Trp, and Tyr for papain (Fig. 3). The general preference for hydrophobic amino acids is consistent with the presence of a hydrophobic pocket at the S2 subsite of clan CA proteases (25). However, although the mini-calpains prefer smaller side chains (Leu, Val, Ile), m-calpain and papain tolerate the large side chains of Trp, Phe, especially if the epoxide group has an (*R,R*) stereochemistry. An m-calpain-specific preference for His at P2 is observed for epoxides bearing an (*R,R*) stereochemistry. A greater difference in specificity between proteases is observed with non-natural amino acids (Fig. 4). Specifically, amino acids 2, 8, 13, 18, 23, and 27 for the (*S,S*)-epoxides and amino acids 2, 4, 5, and 13 for the (*R,R*)-epoxides show potential as either full-length or mini-calpain-specific preferences. (Refer to the supplemental Table 1 for the structures and numerical assignments of the non-natural amino acids).

At position P3, Glu displays a preference  $>2.0$  for  $\mu$ I-II and mI-II G203A, and  $<1$  for m-calpain and papain, indicating a mini-calpain-specific preference for Glu at this position (Fig. 3). Although a strong

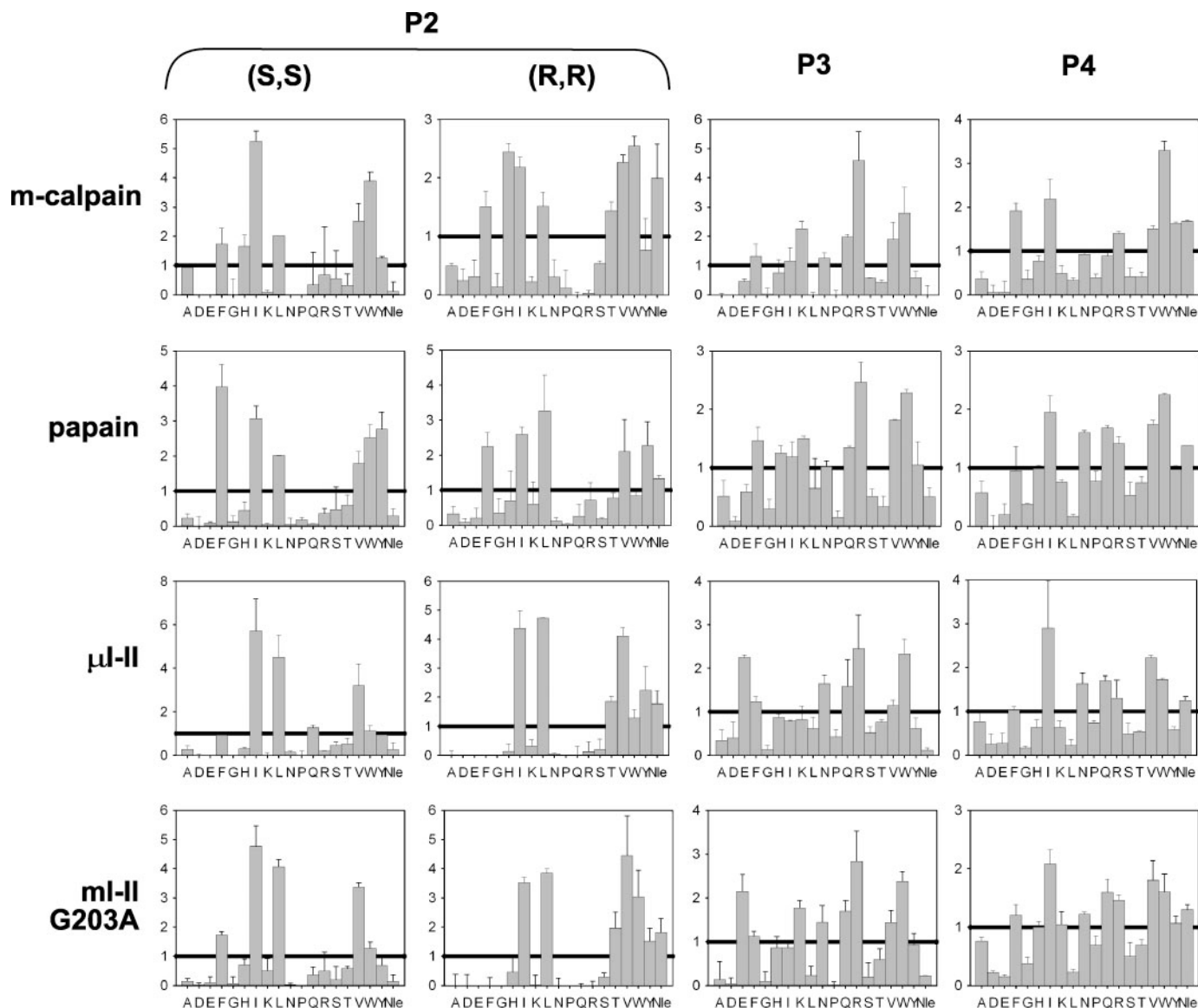
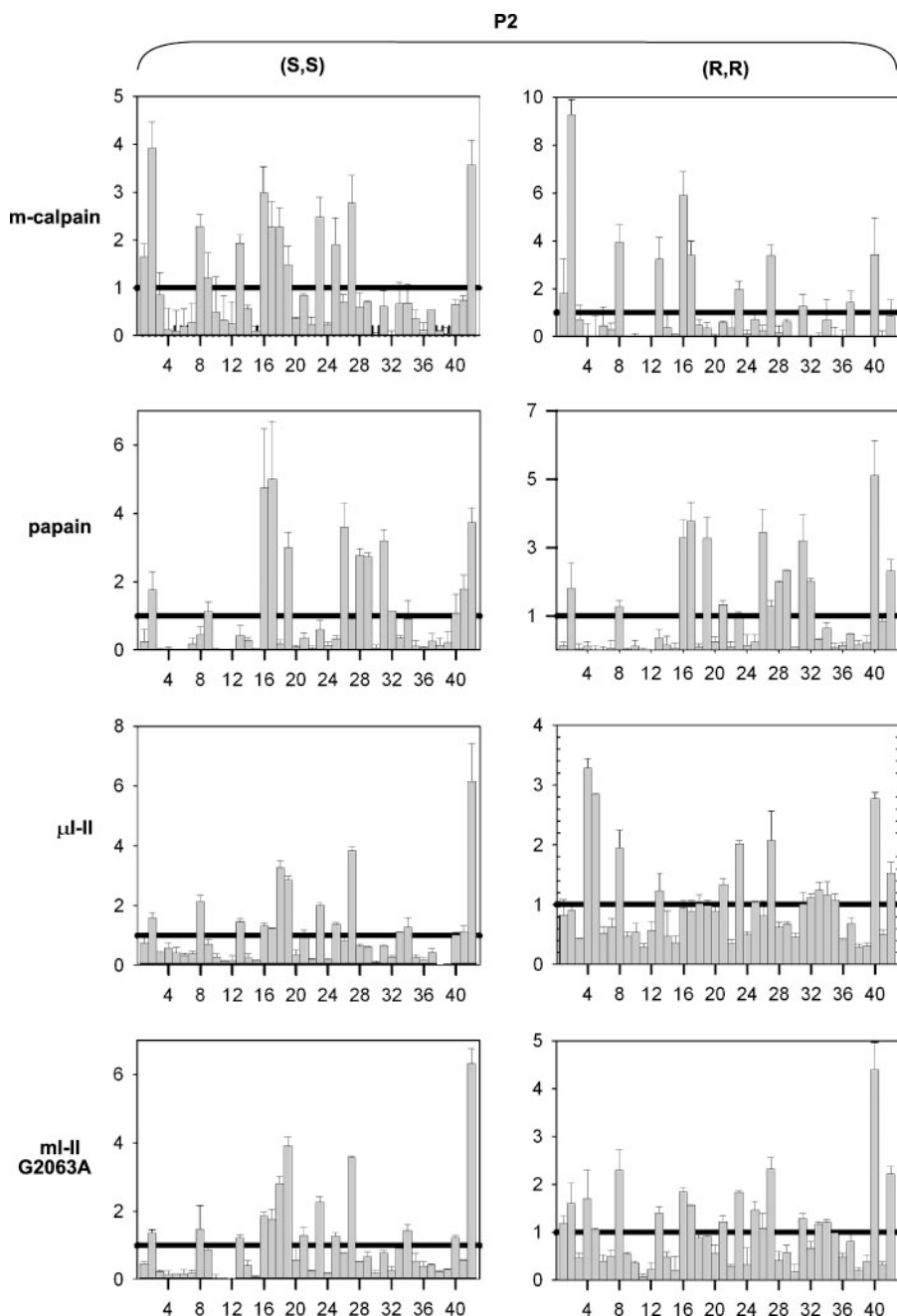


FIGURE 3. **Natural amino acid specificity profiles.** Positional scanning epoxide libraries were screened using m-calpain, papain, and the mini-calpains ( $\mu$ I–II and mI–II G203A). The results are shown as the residue preference (fold inhibition over the average observed for that particular series) for each pool, with the fixed amino acid in the pool on the x axis (*Nle* indicates norleucine). Error bars correspond to the sample standard deviation obtained from duplicate assays.

preference ( $>2.0$ ) for Arg is observed for all three calpain constructs, it is also observed in papain. Similarly, at position P4, no strong calpain-specific preference is observed, although the presence of a tryptophan results in a strong potency toward m-calpain that is understated in the histograms because of the relatively high degree of inhibition observed for all pools of the P4-scanning library. With the exception of a preference for non-natural amino acids 4 and 5 in (*R,R*) stereochemistry for  $\mu$ I–II, the two mini-calpains displayed almost identical specificity. Interestingly, the differences between the mini- and full-length m-calpain preferences at positions P2–P4 suggest that the other domains in full-length calpains can have some impact on the specificity of the protease core.

**Design of Epoxidyl Calpain Inhibitors**—Based on the initial screens, a series of 23 epoxidyl compounds incorporating calpain-specific/preferred amino acids, along with compounds containing amino acid preferences observed from substrate

specificity profiles obtained from a previous study (FFL(*S,S*) and FFL(*R,R*)) (23), were synthesized, and the crude compounds were screened qualitatively for their ability to inhibit m-calpain and  $\mu$ -calpain. The most potent inhibitors of  $\mu$ - and m-calpain share a common Trp-Arg motif at P4–P3 (Fig. 5). To assess which P2 element confers the greatest specificity for calpains, we quantitatively assayed the 10 epoxide compounds containing the Trp-Arg motif (WRX) in a 96-well adapted fluorometric end point assay against m- and  $\mu$ -calpain and the active-site-related and physiologically relevant cathepsins B, L, and K. The compounds demonstrated inhibition potencies (in terms of  $IC_{50}$ ) ranging from 44 to 541 nM for m-calpain and 189–1720 nM for  $\mu$ -calpain. A much broader range of potency was observed against the cathepsins (0.1–35  $\mu$ M for cathepsin B, 0.05–12  $\mu$ M for cathepsin L, and 0.29–54  $\mu$ M for cathepsin K) (Table 1). Upon comparison of the  $IC_{50}$  values, 9 of the 10 WRX compounds (all but WRL(*R,R*)) showed greater specificity



**FIGURE 4. Non-natural amino acid specificity profiles.** The P2-scanning epoxide library was screened using m-calpain, papain, and the mini-calpains ( $\mu$ -II and mI-II G203A). The results are shown as the residue preference (fold inhibition over the average observed for that particular series) for each pool, with the numerical code of the fixed non-natural amino acid in the pool on the x axis (number 42; leucine). The chemical structures for the non-natural amino acids can be found in the Supplemental Material. Error bars correspond to the sample standard deviation obtained from duplicate assays.

toward m-calpain than the cathepsins. Notably, WRH(*R,R*) demonstrated >120-fold better specificity for m-calpain over the cathepsins. Although the compounds were consistently 3–6-fold less potent toward the  $\mu$ -calpain isoform, WRH(*R,R*) still demonstrates >25-fold specificity for  $\mu$ -calpain over the cathepsins. When compared with each other, the two calpain isoforms demonstrated the same relative specificity toward the compounds, consistent with their S2 subsite having similar specificity. Indeed, subsequent screening of the natural and

non-natural P2-scanning libraries against  $\mu$ -calpain resulted in no obvious difference between its profile and that of m-calpain (results not shown).

*WRH(R,R) Is a Calpain-specific Inactivator*—Although  $IC_{50}$  values obtained from end point assays provide a rudimentary way of determining the relative specificity of irreversible inhibitors, the values obtained are highly dependent on preincubation time and experimental methodology and provide no information on the type of inhibition and relative reaction rates. To gain insight into the inhibition of calpains and cathepsins by the lead compound, WRH(*R,R*), we performed a more formal kinetic study using real time fluorescence monitoring. In the presence of WRH(*R,R*), calpain activity is inhibited in a time-dependent fashion (Fig. 6A). This inactivation is significantly more rapid than the intrinsic autolytic inactivation of calpains and results in an eventual complete loss of activity within 5 min even at inhibitor-enzyme stoichiometries of 4:1 (not shown). By determining the rates of inactivation observed at various inhibitor concentrations and subtracting the background rate of autolytic inactivation, second order rate constants of 131,000 and 16,500  $M^{-1} s^{-1}$  for the inactivation of m-calpain and  $\mu$ -calpain, respectively, were determined (Fig. 6B and Table 2). For comparison, a second order inactivation rate constant of 7500  $M^{-1} s^{-1}$  has been reported for the inactivation of m-calpain by E-64 (54); this is a difference of greater than 1 order of magnitude. Conversely, WRH(*R,R*) affected the activity of cathepsins B, L, and K in a time-independent fashion, resulting in a decreased

activity that remains in a steady state, even after 10 min in the presence of 50  $\mu M$  WRH(*R,R*) (Fig. 6C). The absence of a complete loss of enzyme activity, even at inhibitor-enzyme stoichiometries exceeding 50,000:1, signifies that the enzyme is not being irreversibly inactivated, as is the case for calpains, but rather is only reversibly inhibited by the compound. Application of the equations for reversible inhibition kinetics to the steady-state rates obtained at different inhibitor concentrations allowed for the determination of inhibi-

## Epoxide Inhibitors of Calpains

tion constants ( $K_i$ ) for WRH(*R,R*) against the three cathepsins that range from 4.8 to 34  $\mu\text{M}$  (Fig. 6D and Table 2).

**X-ray Structures of WR18(*S,S*) and WR13(*R,R*) Complexes**—Although co-crystallization of the WRH(*R,R*)- $\mu\text{I-II}$  complex yielded large crystals of poor diffraction quality, crystals of  $\mu\text{I-II}$  inactivated by the epoxides WR18(*S,S*) and WR13(*R,R*) were of sufficient quality to study the structure of the complexes by crystallography (Table 3). For both complexes, the



**FIGURE 5. Inhibition by epoxide compounds selected from the library screens.** The inhibitory activity of 23 epoxidyl compounds against m-calpain and  $\mu$ -calpain was monitored by the SDS-PAGE assay. Bands shown are of the Coomassie Blue-stained large 80-kDa subunit of inactive m-calpain C105S. Inhibitor notation is given in the format P4-P3-P2, with a regular font indicating (*S,S*) stereochemistry and a **bold underlined font** indicating (*R,R*) stereochemistry. Controls show the 80-kDa band in the absence of digestion (–) and in the absence of inhibition (+). The inhibitor concentrations used are 10  $\mu\text{M}$  (m-calpain) and 1  $\mu\text{M}$  ( $\mu$ -calpain). In this particular figure, the m-calpain assay was performed in *cis* mode (autolysis).

**TABLE 1**

### Calpain specificity of the WRX epoxides relative to cathepsins B, L, and K as obtained from end point fluorometric assays

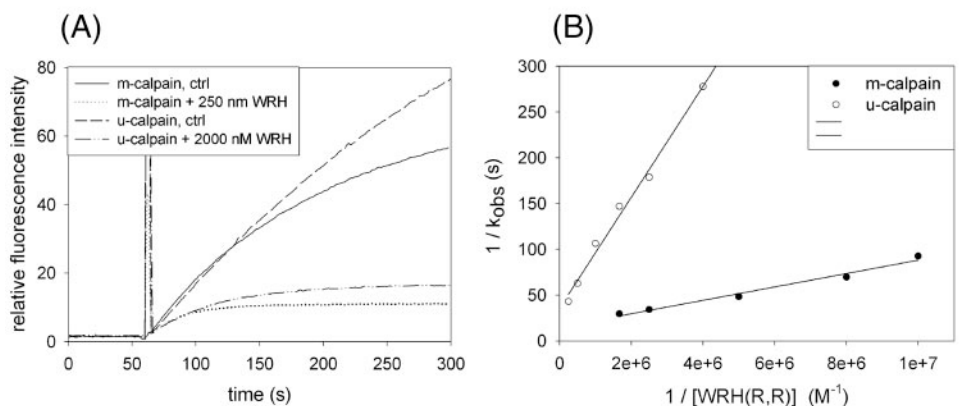
Ten epoxide compounds containing a Trp-Arg motif at P4-P3 were assayed for potency using fluorimetric end point assays adapted to a 96-well plate format. Data represents the mean  $\pm$  S.D. of triplicate experiments. Specificity was calculated as the ratio of the determined  $\text{IC}_{50}$  values between protease pairs, with values  $>20$  shown in boldface type.

Compound	m-Calpain	$\mu$ -Calpain	Cathepsin B	Cathepsin L	Cathepsin K
WR2( <i>S,S</i> )					
IC <sub>50</sub> (nM)	44 $\pm$ 7	189 $\pm$ 46	480 $\pm$ 100	310 $\pm$ 50	490 $\pm$ 9
m-Calpain-specific		4.3	11	7.0	11
$\mu$ -Calpain-specific	0.23		2.5	1.6	2.6
WR8( <i>S,S</i> )					
IC <sub>50</sub> (nM)	62 $\pm$ 7	415 $\pm$ 84	510 $\pm$ 120	1090 $\pm$ 100	2300 $\pm$ 340
m-Calpain-specific		6.7	8.2	18	37
$\mu$ -Calpain-specific	0.15		1.2	2.6	5.5
WR18( <i>S,S</i> )					
IC <sub>50</sub> (nM)	112 $\pm$ 17	333 $\pm$ 95	1080 $\pm$ 220	1190 $\pm$ 300	2240 $\pm$ 600
m-Calpain-specific		3.0	9.7	11	20
$\mu$ -Calpain-specific	0.34		3.3	3.6	6.7
WR23( <i>S,S</i> )					
IC <sub>50</sub> (nM)	119 $\pm$ 20	323 $\pm$ 67	3000 $\pm$ 790	370 $\pm$ 100	1680 $\pm$ 490
m-Calpain-specific		2.7	<b>25</b>	3.1	14
$\mu$ -Calpain-specific	0.37		9.3	1.2	5.2
WR27( <i>S,S</i> )					
IC <sub>50</sub> (nM)	46 $\pm$ 1	193 $\pm$ 56	100 $\pm$ 20	50 $\pm$ 30	320 $\pm$ 62
m-Calpain-specific		4.2	2.1	1.2	6.9
$\mu$ -Calpain-specific	0.24		0.51	0.28	1.7
WR2( <i>R,R</i> )					
IC <sub>50</sub> (nM)	113 $\pm$ 7	437 $\pm$ 68	1.3 $\times 10^4 \pm 0.4$	840 $\pm$ 320	8830 $\pm 1500$
m-Calpain-specific		3.9	<b>120</b>	7.4	<b>78</b>
$\mu$ -Calpain-specific	0.26		<b>30</b>	1.9	<b>20</b>
WR13( <i>R,R</i> )					
IC <sub>50</sub> (nM)	256 $\pm$ 37	784 $\pm$ 130	3460 $\pm$ 480	430 $\pm$ 50	4600 $\pm$ 826
m-Calpain-specific		3.1	14	1.7	18
$\mu$ -Calpain-specific	0.33		4.4	0.55	<b>5.9</b>
WRH( <i>R,R</i> )					
IC <sub>50</sub> (nM)	101 $\pm$ 9	459 $\pm$ 39	3.5 $\times 10^4 \pm 0.4$	1.2 $\times 10^4 \pm 0.2$	5.4 $\times 10^4 \pm 1.8$
m-Calpain-specific		4.6	<b>350</b>	<b>120</b>	<b>530</b>
$\mu$ -Calpain-specific	0.22		77	<b>26</b>	<b>120</b>
WRW( <i>R,R</i> )					
IC <sub>50</sub> (nM)	390 $\pm$ 87	884 $\pm$ 104	2.1 $\times 10^4 \pm 0.5$	640 $\pm$ 230	1.3 $\times 10^4 \pm 0.2$
m-Calpain-specific		2.3	<b>53</b>	1.6	<b>33</b>
$\mu$ -Calpain-specific	0.44		<b>23</b>	0.72	14
WRL( <i>R,R</i> )					
IC <sub>50</sub> (nM)	541 $\pm$ 56	1720 $\pm$ 90	4930 $\pm$ 120	70 $\pm$ 50	290 $\pm$ 60
m-Calpain-specific		3.2	9.1	0.13	0.54
$\mu$ -Calpain-specific	0.31		2.9	0.04	0.17

His-272. However, the effect of the different stereochemistry of the two ligands is apparent in the positions of the remainder of the warhead as it extends across the S1 subsite of the active-site cleft. Although both the amide oxygen of the (*R,R*)- and the (*S,S*)-warheads form a hydrogen bond with the backbone amide of Gly-208, only the amide nitrogen of the (*R,R*)-warhead forms a second hydrogen bond with the backbone carbonyl of Gly-271. The P2 moieties of both compounds fit into the

S2 hydrophobic pocket, although the  $\alpha$ -carbon of the allylglycine of WR13(*R,R*) is positioned about 1.2 Å deeper into the pocket than the  $\alpha$ -carbon of the  $\gamma$ -cyano- $\alpha$ -aminobutyric acid residue of WR18(*S,S*), and the P2 side chains extend from their  $\alpha$ -carbons at different angles (Fig. 8). Additionally, the P2  $\gamma$ -cyano group of WR18(*S,S*) forms a hydrogen bond to a water molecule (HOH70) stabilized in the S2 pocket by the acidic side chain of Glu-349 and the backbone amide of Thr-210 (Fig. 7, C and D, and Fig. 8).

## Calpains



## Cathepsins

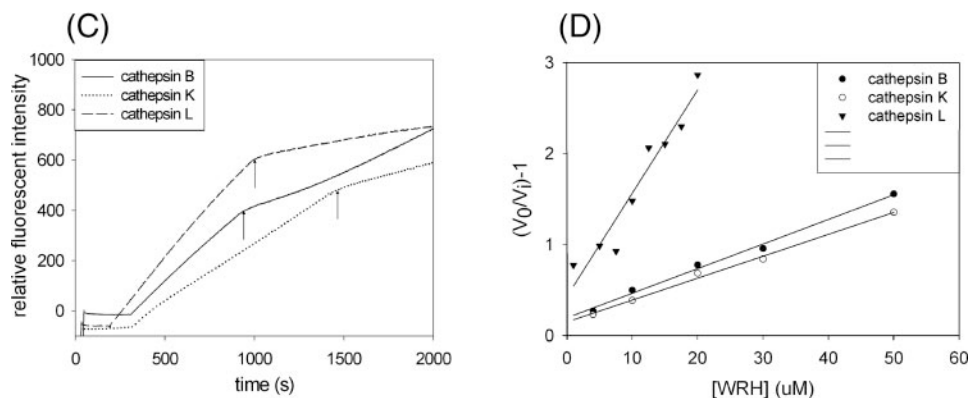


**FIGURE 6. Inhibition of calpains and cathepsins by WRH(*R,R*).** *A*, calpain-catalyzed product formation was monitored in real time using fluorescence assay as described under "Experimental Procedures." The reaction is initiated by the simultaneous addition of  $\text{Ca}^{2+}$  and 250 nM (for m-calpain) or 2  $\mu\text{M}$  (for  $\mu$ -calpain) WRH(*R,R*) at  $t = 60$  s. The control reactions lack WRH(*R,R*) and therefore represent the autolytic inactivation of the enzyme. *B*, linear regression of a  $1/k_{\text{obs}}$  versus  $1/[I]$  plot is used to calculate the kinetic constants of inactivation ( $k_2$  and  $K_i$ ) for m-calpain ( $\bullet$ ) and  $\mu$ -calpain ( $\circ$ ). *C*, effect of WRH(*R,R*) on cathepsin-catalyzed product formation is monitored similarly to calpains, except that the reaction is initiated by the addition of enzyme. Once steady state is achieved, 20  $\mu\text{M}$  (for cathepsin L) or 50  $\mu\text{M}$  (for cathepsins B and K) WRH(*R,R*) is added, as indicated by the arrows. *D*, linear regression of a  $(V_0/V_i) - 1$  versus  $[I]$  plot, where  $V_0$  and  $V_i$  are initial and inhibited reaction rates, is used to calculate the inhibition constant ( $K_i$ ) for cathepsin B ( $\bullet$ ), L ( $\blacktriangledown$ ), and K ( $\circ$ ). Each data point represents the average of replicate assays performed at each inhibitor concentration.

**TABLE 2**

### Summary of inhibition kinetics of WRH(*R,R*)

Kinetic constants were derived from linear regression plots shown in Fig. 6, *B* and *D*. Reported error margins represent the standard deviation obtained from the linear regression of the data.

Protease	Type of inhibition	$K_i$	$k_2$	$k_2/K_i$
		$\mu\text{M}$	$\text{s}^{-1}$	$\text{M}^{-1} \text{s}^{-1}$
m-Calpain	Irreversible	$0.518 \pm 180$	$0.068 \pm 0.016$	$131,000 \pm 50,000$
$\mu$ -Calpain	Irreversible	$1.69 \pm 0.39$	$0.028 \pm 0.005$	$16,500 \pm 5000$
Cathepsin B	Reversible	$34 \pm 2$	/	/
Cathepsin K	Reversible	$20 \pm 2$	/	/
Cathepsin L	Reversible	$4.8 \pm 0.8$	/	/

## DISCUSSION

The development of calpain-specific inhibitors used to lessen the damage done in reperfusion injury after ischemic episodes and in longer term pathologies, such as neurodegeneration and cataract formation, has yielded limited results in the past. This task is made difficult by the ability of the active site of calpain to accommodate a wide variety of residues in all subsites except P2, where its specificity is similar to other related cysteine proteases (23, 55). Combinatorial approaches have provided opportunities for sampling large numbers of systematically substituted compounds for their inhibitory capabilities once an appropriate high throughput assay is developed.

Screening the epoxidyl positional scanning libraries provided the specificity profiles for three calpain constructs as well as papain. The propensity for hydrophobic amino acids, such as Ile and Val, at the P2 position typical of clan CA proteases like calpains and papain is apparent from these specificity profiles. However, additional preferences were observed with the epoxidyl compounds that were not previously predicted from studies on the peptide substrate specificity of calpains (23, 55). In particular, large amino acids such as Trp, Phe,

**TABLE 3**  
Summary from data collection and structure refinement

Crystal parameters	$\mu\text{I-II-WR18}(S,S)$ complex		$\mu\text{I-II-WR13}(R,R)$ complex	
Space group	P2 <sub>1</sub> 2 <sub>1</sub> 2 <sub>1</sub>		P2 <sub>1</sub> 2 <sub>1</sub> 2 <sub>1</sub>	
<i>a</i> (Å)	40.554		40.37	
<i>b</i> (Å)	70.59		70.06	
<i>c</i> (Å)	110.19		110.74	
Data collection statistics	Total	Outer shell	Total	Outer shell
Resolution range (Å)	110.4–2.04	2.12–2.04	59.3–2.04	2.12–2.04
Measured reflections	61,891	5848	164,545	8431
Unique reflections	17,455	1808	19,556	2235
Completeness (%)	88.1	59.4	99.3	72.4
<i>I</i> / $\sigma$ <i>I</i>	14.6	4.1	11.0	3.1
<i>R</i> <sub>merge</sub> <sup>a</sup> (%)	7.9	32.5	13.9	45.6
Refined structural model	Total	Outer shell	Total	Outer shell
Resolution range	110.4–2.04	2.09–2.04	59.3–2.04	2.09–2.04
Size of free reflection set (%)	5.0	5.0	5.1	5.1
<i>R</i> <sub>work</sub> <sup>b</sup>	18.4	19.8	18.4	18.9
<i>R</i> <sub>free</sub>	25.1	35.2	24.7	28.8
No. of protein/solvent/Ca <sup>2+</sup> atoms (no H)	2631/126/2		2634/153/2	
Bond angle r.m.s.d. <sup>c</sup> (degree)	1.68		1.66	
Bond length r.m.s.d. (Å)	0.019		0.017	
Average <i>B</i> -factor (Å <sup>2</sup> )	18.4		16.7	
<i>B</i> -factor from Wilson plot (Å <sup>2</sup> )	19.4		17.3	

<sup>a</sup>  $R_{\text{merge}} = \sum |I_j - \langle I \rangle| / \sum I_j$ , where  $I_j$  are individual measurements for any one reflection and  $\langle I \rangle$  is the average intensity of the symmetry equivalent reflections.

<sup>b</sup>  $R_{\text{cryst}} = \sum |F_o - F_c| / \sum F_o$ ;  $F_o$  and  $F_c$  are observed and calculated structure factor amplitudes, respectively.

<sup>c</sup> r.m.s.d. indicates root mean square deviation.

and His at the P2 positions are preferred by calpain in reaction with the epoxide inhibitors but are selected against at the same position in substrates. This observation can be explained by the different chemical frameworks of peptide substrates and the epoxide compounds. The peptide backbone of the epoxide compounds (C to N in the P4–P2 direction) extends in the reverse orientation to that adopted by a peptidyl substrate (N to C in the P4–P2 direction) (Fig. 1). This allows the amino acid side chains to project in a different orientation within the subsites of the protease than they would in a substrate, and can possibly result in the accommodation of amino acids that would otherwise have a poor fit. Previous inhibitor-bound structures demonstrated that substrate analogs leupeptin, SNJ-1715, and SNJ-1945 form two hydrogen bonds between the peptide backbone and the calpain active site at the P2 position (25, 27). In contrast, the epoxide-inactivated structures show either a single (for the (*R,R*)-epoxide, Fig. 7D) or no hydrogen bonds (for the (*S,S*)-epoxide, Fig. 7C) formed between the inhibitor backbone and the active site at the P2 position, suggesting a greater freedom of movement of the P2 side chain within the S2-binding site when the residue is in the structural context of these epoxidyl compounds. The dependence of the specificity profile on the stereochemistry of the epoxide further highlights the importance of subtle changes in side chain orientation on specificity. Therefore, specificity profiles arising from the screening of compounds of different structural nature, such as peptide substrates and epoxidyl inactivators, will likely not be identical.

The use of mini-calpains as surrogates for the whole enzyme circumvents many of the problems that make the full-length enzymes difficult with which to work. Although whole calpains have not yet been crystallized in the presence of Ca<sup>2+</sup>, mini-calpains can be crystallized in their active calcium-bound conformation and allow for structure-based design of active-site inhibitors. However, the differences observed between the

specificity profiles of the mini- and full-length calpain illustrate some potential limitations of this approach and emphasize the importance of co-validating results observed with the mini-calpains on their full-length counterparts. Specificity for residues at the P3 and P4 positions is more likely to be misrepresented by mini-calpains. These positions are far enough from the active-site cysteine that they may be influenced by other domains (notably domain III) in the full-length enzyme. The absence of electron density in the crystal structure of the  $\mu\text{I-II}$  complexes corresponding to the P4-Trp, along with the absence of distinct preference for this residue from the P4 library screens when using  $\mu\text{I-II}$  or  $\text{mI-II}$  G203A, suggests that this particular preference in m-calpain may be the result of interactions with additional domains of the full-length enzyme not found in the mini-calpain.

Consistent with the known active-site specificity, most active-site inhibitors of calpains contain a small aliphatic amino acid, commonly leucine or valine, as the P2 element (16). These residues, although providing potency toward calpains, are not very selective as they are also accommodated by the hydrophobic pocket of other clan CA proteases (56). For example, the first natural epoxide inhibitor, E-64, contains a leucine at the P2 positions and is used as a broad range inhibitor of clan CA proteases (28). The preference of calpains for histidine at the P2 position, although likely observed strictly in the context of an epoxide inhibitor with an (*R,R*) stereochemistry, presents a novel type of chemical entity to interact with the S2 subsite. The presence of a histidine at the P2 positions resulted in a significantly higher specificity for the epoxide series containing a WR motif at the P4–P3 position, suggesting that it can interact better with structural elements of the active site of calpain that are not present in the other proteases tested. Although the nature of the inhibition of cathepsins B, L, and K by WRH(*R,R*) suggests that the compound interacts with the active site of these enzymes, the absence of inactivation implies that the interac-

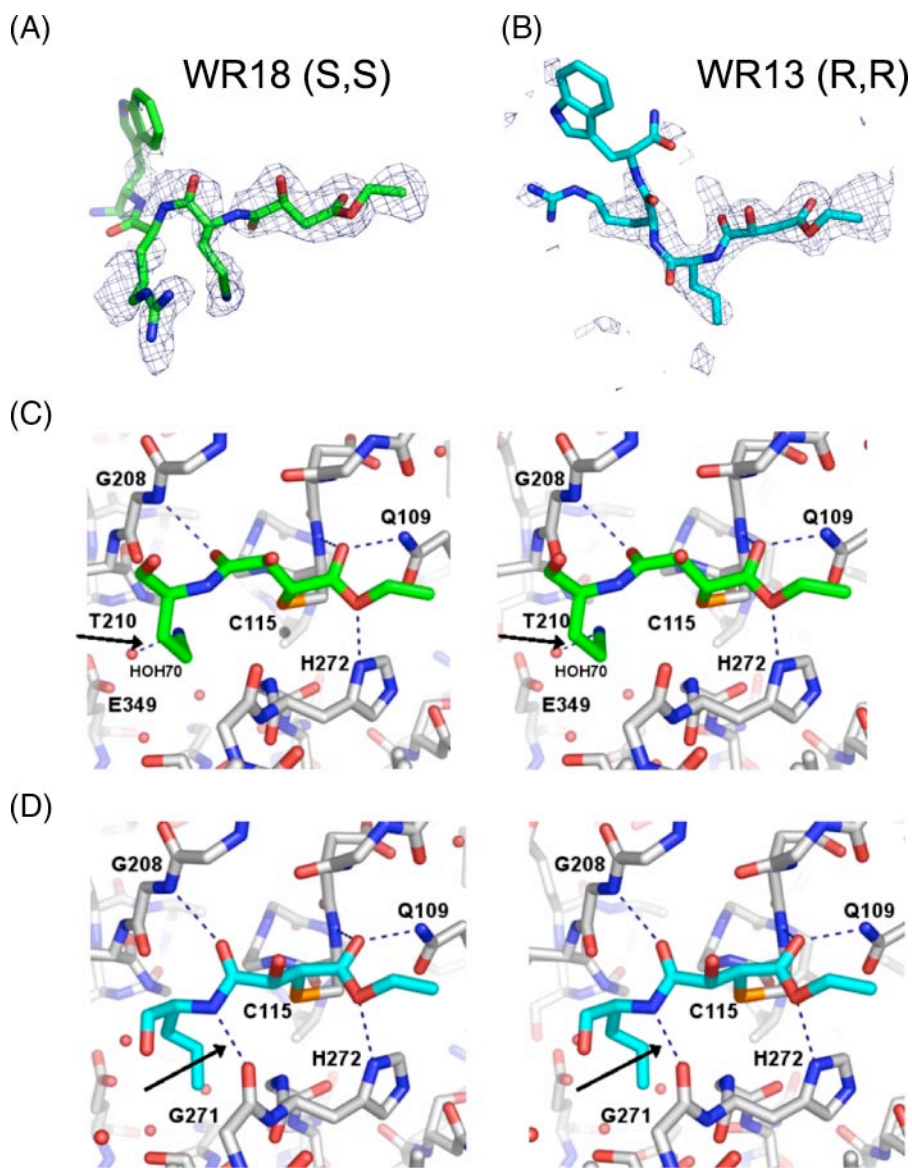


FIGURE 7. Crystal structures of  $\mu$ I–II inactivated by WR18(*S,S*) and WR13(*R,R*). *A* and *B*, fitted electron density of WR18(*S,S*) and WR13(*R,R*), respectively. The observed electron density for the ligands is shown by an  $F_o - F_c$  (omit) map calculated for the structures omitting the ligands and contoured at  $2\sigma$ . *C* and *D*, stereo images demonstrating the hydrogen bonds formed by WR18(*S,S*) and WR13(*R,R*), respectively. All polar bonds shorter than 3.2 Å are shown by dashes. Carbon atoms of the polypeptide are colored white, and water molecules are shown as red spheres. The flexible P3–Arg and P4–Trp moieties of the ligands were omitted for clarity. Arrows point to the hydrogen bond between WR18(*S,S*) and a water molecule within the S2 pocket in *C* and to the (*R,R*)-epoxide specific hydrogen bond between the P2 backbone amide of WR13(*R,R*) and Gly-271 in *D*.

tion is such that the epoxide group is not in a position to react with the nucleophilic thiol of the active site. Structural studies with WRH(*R,R*) might reveal the differences between the active sites of the two protease families that result in this distinct difference in specificity, and this information could be applied to design inhibitors with improved selectivity.

Preferences at P2 were dependent on the stereochemistry of the epoxide for all four proteases used in library screening, illustrating the utility of this variable in generating specificity (35). Attempts have been made to model epoxides of different stereochemistry into the active site of the SARS coronavirus main peptidase (57), and previous work with cathepsin B led to the suggestion that an (*R,R*) configuration of the epoxide favors

binding at the P-primed positions (58). The crystal structures of  $\mu$ I–II inactivated by both an (*S,S*)- and an (*R,R*)-epoxide warhead provide structural insights on epoxide stereochemistry and ligand binding that contradicts the latter hypothesis. In both the (*S,S*)- and (*R,R*)-inactivated structures, the ethyl ester groups occupy nearly identical positions at the S1' subsite (Fig. 8), suggesting that these primed side interactions form an “anchor” that is independent of the stereochemistry of the warhead. Instead, the epoxide stereochemistry appears to affect inhibition specificity by affecting the position and orientation of the P2 residues, allowing for different potential interactions to form within the S2 pocket. This difference in the position of the P2 residue may be related to the ability of the P2 amide nitrogen of an (*R,R*)-epoxide to form a hydrogen bond with the backbone carbonyl oxygen of Gly-271, resulting in the P2  $\alpha$ -carbon being positioned deeper within the S2 pocket compared with epoxides with (*S,S*) stereochemistry. However, because these structures represent the inactivator after nucleophilic attack has occurred, the state of the compound prior to covalent bond formation can only be inferred.

Although the P3- and P4-scanning libraries contained only (*S,S*) stereochemistry, the P4–Trp P3–Arg motif inferred from the screens was applied to generate inhibitors of both (*S,S*) or (*R,R*) stereochemistry. The similar potency of these inhibitors regardless of their stereochemical configuration is consistent with

specificity at the P3 and P4 positions being less influenced by the epoxide stereochemistry because of their more distal position to the warhead.

The structure of  $\mu$ I–II complexed with E-64, an epoxide inhibitor with an (*S,S*) stereochemistry and a P2 leucine, was determined previously (25) and provides a model for direct comparison with WR13(*R,R*) and WR18(*S,S*)-complexed structures. The P1' carboxylate of E-64 occupies the same position as the esters of both ligands (Fig. 8), supporting the notion that this portion of the warhead anchors the inhibitor in the active site. The P2 backbone moiety (carbonyl carbon,  $\alpha$ -carbon, and amide nitrogen) and the  $\beta$ - and  $\gamma$ -carbons of the P2 leucine of E-64 superimpose over the corresponding atoms of WR18(*S,S*)

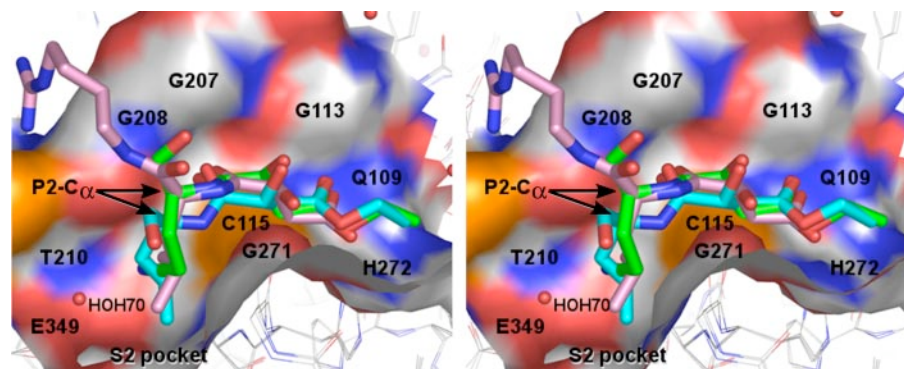


FIGURE 8. **Structural overlap of three epoxide-derived ligands.** The overlap of WR18(*S,S*), WR13(*R,R*) and E-64 was obtained by the structural alignment of the  $\alpha$ -carbons of the polypeptide chain. The color scheme is as in Fig. 7, with carbon atoms of E-64 in pink. The active site for the WR18(*S,S*) complex is shown as a surface. Arrows point to the position of the  $\alpha$ -carbons of the P2 residues. The flexible P3-Arg and P4-Trp moieties of WR13(*R,R*) and WR18(*S,S*) were omitted for clarity.

but not with those of WR13(*R,R*), and the P2 backbone amide nitrogen of E-64 does not form a hydrogen bond with Gly-271, consistent with the position of these atoms being dictated by the (*S,S*) stereochemistry of the epoxide. Two significant differences in the hydrogen-bonding pattern of E-64 are the absence of a hydrogen bond between the amide carbonyl of the warhead and Gly-208, and the presence of a hydrogen bond between the hydroxyl group formed from the opening of the epoxide and the carbonyl oxygen of Gly-271, indicating a slightly different mode of binding from WR13(*R,R*) and WR18(*S,S*) that appears to have no impact on the remainder of the ligand.

In addition to providing insight into epoxide-specific stereochemistry, the epoxide-inactivated structures provide more clues into active-site interactions of calpains with relevance to inhibitor design. First, as observed in a previously published  $\mu$ I-II-SNJ-1945 structure, residues 256–261 of the domain II flexible loop of  $\mu$ I-II have little to no electron density to which to fit (not shown). This confirms our previously proposed hypothesis that the presence of a ligand in the S1' subsite of calpains (in this case the ethyl ester group of the epoxysuccinyl group) results in the displacement of Glu-261 from the subsite and an extended open conformation of the domain II flexible loop that gates the active site (25, 27). Although the E-64-complexed structure displays the Glu-261 side chain in the vicinity of the S1' subsite, the electron density for it is absent (not shown), suggesting that the presence of carboxylic acid group at P1' is sufficient to displace the loop.

Second, the WR18(*S,S*)-bound structure provides the first instance of a hydrogen bond occurring within the S2 pocket of calpain. This interaction, formed between the  $\gamma$ -cyano group of non-natural amino acid 18 and a water molecule at the periphery of the S2 pocket, could potentially be replicated in other inhibitors to provide a stronger and potentially more specific interaction at the S2 subsites over the short hydrophobic amino acids typically used at this position in calpain inhibitors. The water molecule involved, held by Glu-349 and Thr-210, is conserved in all  $\mu$ I-II structures to date and thus appears to be a fixed feature of the calpain active site. Comparison of the calpain specificity obtained for compounds WR18(*S,S*) and WR13(*R,R*) over cathepsin L

and K hints at the improvement in specificity that could be obtained by incorporating a properly positioned hydrogen bond acceptor at the P2 position.

Our data will help guide ongoing efforts at designing calpain-specific inhibitors and activity-based probes that discriminate among overlapping cathepsin-like proteases. Because labeling of an enzyme by an activity-based probe is dependent on its irreversible modification, the calpain-selective modification of WRH(*R,R*) suggests an ideal lead candidate from which to generate calpain-specific

probes. Such inhibitors and probes will be invaluable tools to tackle the pathophysiological roles of this pharmacologically important family of signaling proteases.

*Acknowledgments*—We thank Sherry Gauthier and Simon Baxter for technical assistance; Zongchao Jia for providing the facilities for x-ray crystallography data collection; Michael E. Nesheim for use of the fluorescent plate reader; and David Zechel and Derek Pratt from the Department of Chemistry at Queen's University for valuable discussion of inactivation kinetics. We also thank Dr. Robert Menard for the gift of cathepsin K.

## REFERENCES

- Lee, M. S., Kwon, Y. T., Li, M., Peng, J., Friedlander, R. M., and Tsai, L. H. (2000) *Nature* **405**, 360–364
- Toyota, H., Yanase, N., Yoshimoto, T., Moriyama, M., Sudo, T., and Mizuguchi, J. (2003) *Cancer Lett.* **189**, 221–230
- Glading, A., Lauffenburger, D. A., and Wells, A. (2002) *Trends Cell Biol.* **12**, 46–54
- Janossy, J., Ubezio, P., Apati, A., Magocsi, M., Tompa, P., and Friedrich, P. (2004) *Biochem. Pharmacol.* **67**, 1513–1521
- Neumar, R. W., Xu, Y. A., Gada, H., Guttmann, R. P., and Siman, R. (2003) *J. Biol. Chem.* **278**, 14162–14167
- Kambe, A., Yokota, M., Saido, T. C., Satokata, I., Fujikawa, H., Tabuchi, S., Kamitani, H., and Watanabe, T. (2005) *Brain Res.* **1040**, 36–43
- Richard, I., Broux, O., Allamand, V., Fougerousse, F., Chiannilkulchai, N., Bourg, N., Brenguier, L., Devaud, C., Pasturaud, P., Roudaut, C., and Hillaire, D., Passos-Bueno, M.-R., Zatz, M., Tischfield, J. A., Fardeau, M., Jackson, C. E., Cohen, D., and Beckmann, J. S. (1995) *Cell* **81**, 27–40
- Chou, F. L., Angelini, C., Daentl, D., Garcia, C., Greco, C., Hausmanowa-Petrusewicz, I., Fidzińska, A., Wessel, H., and Hoffman, E. P. (1999) *Neurology* **52**, 1015–1020
- Cox, N. J., Hayes, M. G., Roe, C. A., Tsuchiya, T., and Bell, G. I. (2004) *Diabetes* **53**, S19–S25
- Yoshikawa, Y., Mukai, H., Hino, F., Asada, K., and Kato, I. (2000) *Jpn. J. Cancer Res.* **91**, 459–463
- Hong, S. C., Goto, Y., Lanzino, G., Soleau, S., Kassell, N. F., and Lee, K. S. (1994) *Stroke* **25**, 663–669
- Bartus, R. T., Hayward, N. J., Elliott, P. J., Sawyer, S. D., Baker, K. L., Dean, R. L., Akiyama, A., Straub, J. A., Harbeson, S. L., and Li, Z. (1994) *Stroke* **25**, 2265–2270
- Mathur, P., Gupta, S. K., Wegener, A. R., Breipohl, W., Ahrend, M. H., Sharma, Y. D., Gupta, Y. K., and Vajpayee, R. B. (2000) *Curr. Eye Res.* **21**, 926–933
- Huang, Y., and Wang, K. K. (2001) *Trends Mol. Med.* **7**, 355–362

15. Turk, D., Guncar, G., Podobnik, M., and Turk, B. (1998) *Biol. Chem.* **379**, 137–147
16. Wang, K. K., and Yuen, P. W. (1997) *Adv. Pharmacol.* **37**, 117–152
17. Figueiredo-Pereira, M. E., Banik, N., and Wilk, S. (1994) *J. Neurochem.* **62**, 1989–1994
18. Tsujinaka, T., Kajiwara, Y., Kambayashi, J., Sakon, M., Higuchi, N., Tanaka, T., and Mori, T. (1988) *Biochem. Biophys. Res. Commun.* **153**, 1201–1208
19. Hiwasa, T., Sawada, T., and Sakiyama, S. (1990) *Carcinogenesis* **11**, 75–80
20. Chatterjee, S., Gu, Z. Q., Dunn, D., Tao, M., Josef, K., Tripathy, R., Bihovsky, R., Senadhi, S. E., O'Kane, T. M., McKenna, B. A., Mallya, S., Ator, M. A., Bozyczko-Coyne, D., Siman, R., and Mallamo, J. P. (1998) *J. Med. Chem.* **41**, 2663–2666
21. Moldoveanu, T., Hosfield, C. M., Lim, D., Elce, J. S., Jia, Z., and Davies, P. L. (2002) *Cell* **108**, 649–660
22. Moldoveanu, T., Jia, Z., and Davies, P. L. (2004) *J. Biol. Chem.* **279**, 6106–6114
23. Cuerrier, D., Moldoveanu, T., and Davies, P. L. (2005) *J. Biol. Chem.* **280**, 40632–40641
24. Moldoveanu, T., Hosfield, C. M., Lim, D., Jia, Z., and Davies, P. L. (2003) *Nat. Struct. Biol.* **10**, 371–378
25. Moldoveanu, T., Campbell, R. L., Cuerrier, D., and Davies, P. L. (2004) *J. Mol. Biol.* **343**, 1313–1326
26. Li, Q., Hanzlik, R. P., Weaver, R. F., and Schonbrunn, E. (2006) *Biochemistry* **45**, 701–708
27. Cuerrier, D., Moldoveanu, T., Inoue, J., Davies, P. L., and Campbell, R. L. (2006) *Biochemistry* **45**, 7446–7452
28. Barrett, A. J., Kembhavi, A. A., Brown, M. A., Kirschke, H., Knight, C. G., Tamai, M., and Hanada, K. (1982) *Biochem. J.* **201**, 189–198
29. Greenbaum, D., Medzihradzky, K. F., Burlingame, A., and Bogyo, M. (2000) *Chem. Biol.* **7**, 569–581
30. Matsumoto, K., Mizoue, K., Kitamura, K., Tse, W. C., Huber, C. P., and Ishida, T. (1999) *Biopolymers* **51**, 99–107
31. Bogyo, M., Verhelst, S., Bellingard-Dubouchaud, V., Toba, S., and Greenbaum, D. (2000) *Chem. Biol.* **7**, 27–38
32. Schaschke, N., Assfalg-Machleidt, I., Machleidt, W., and Moroder, L. (1998) *FEBS Lett.* **421**, 80–82
33. Katunuma, N., Murata, E., Kakegawa, H., Matsui, A., Tsuzuki, H., Tsuge, H., Turk, D., Turk, V., Fukushima, M., Tada, Y., and Asao, T. (1999) *FEBS Lett.* **458**, 6–10
34. Greenbaum, D. C., Arnold, W. D., Lu, F., Hayrapetian, L., Baruch, A., Krumrine, J., Toba, S., Chehade, K., Bromme, D., Kuntz, I. D., and Bogyo, M. (2002) *Chem. Biol.* **9**, 1085–1094
35. James, K. E., Asgian, J. L., Li, Z. Z., Ekici, O. D., Rubin, J. R., Mikolajczyk, J., Salvesen, G. S., and Powers, J. C. (2004) *J. Med. Chem.* **47**, 1553–1574
36. Moldoveanu, T., Hosfield, C. M., Jia, Z., Elce, J. S., and Davies, P. L. (2001) *Biochim. Biophys. Acta* **1545**, 245–254
37. Elce, J. S., Hegadorn, C., Gauthier, S., Vince, J. W., and Davies, P. L. (1995) *Protein Eng.* **8**, 843–848
38. Verhelst, S. H., and Bogyo, M. (2005) *Chembiochem* **6**, 824–827
39. Barrett, A. J., and Salvesen, G. (eds) (1986) *Proteinase Inhibitors*, pp. 23–51, Elsevier Science Publishers B.V., Amsterdam
40. Crawford, C., Mason, R. W., Wikstrom, P., and Shaw, E. (1988) *Biochem. J.* **253**, 751–758
41. Powers, J. C., Asgian, J. L., Ekici, O. D., and James, K. E. (2002) *Chem. Rev.* **102**, 4639–4750
42. Barrett, A. J., Kirschke, H., Cathepsin, B., Cathepsin, H., and Cathepsin, L. (1981) *Methods Enzymol.* **80**, 535–561
43. Wiczczak, E., Jankowska, E., Rodziejewicz-Motowidlo, S., Gieldon, A., Lagiewka, J., Grzonka, Z., Abrahamson, M., Grubb, A., and Bromme, D. (2005) *J. Pept. Res.* **66**, 1–11
44. Mason, R. W., Green, G. D., and Barrett, A. J. (1985) *Biochem. J.* **226**, 233–241
45. Leslie, A. G. (2006) *Acta Crystallogr. Sect. D. Biol. Crystallogr.* **62**, 48–57
46. Potterton, E., McNicholas, S., Krissinel, E., Cowtan, K., and Noble, M. (2002) *Acta Crystallogr. Sect. D. Biol. Crystallogr.* **58**, 1955–1957
47. Vagin, A. A., and Isupov, M. N. (2001) *Acta Crystallogr. Sect. D. Biol. Crystallogr.* **57**, 1451–1456
48. Murshudov, G. N., Vagin, A. A., Lebedev, A., Wilson, K. S., and Dodson, E. J. (1999) *Acta Crystallogr. Sect. D Biol. Crystallogr.* **55**, 247–255
49. McRee, D. E. (1999) *J. Struct. Biol.* **125**, 156–165
50. Schuttelkopf, A. W., and van Aalten, D. M. (2004) *Acta Crystallogr. Sect. D. Biol. Crystallogr.* **60**, 1355–1363
51. DeLano, W. L. (2003) *PyMOL Molecular Graphics System*, Version 0.99rc6, DeLano Scientific LLC, San Carlos, CA
52. Greenbaum, D., Baruch, A., Hayrapetian, L., Darula, Z., Burlingame, A., Medzihradzky, K. F., and Bogyo, M. (2002) *Mol. Cell. Proteomics* **1**, 60–68
53. Greenbaum, D. C., Baruch, A., Grainger, M., Bozdech, Z., Medzihradzky, K. F., Engel, J., DeRisi, J., Holder, A. A., and Bogyo, M. (2002) *Science* **298**, 2002–2006
54. Parkes, C., Kembhavi, A. A., and Barrett, A. J. (1985) *Biochem. J.* **230**, 509–516
55. Tompa, P., Buzder-Lantos, P., Tantos, A., Farkas, A., Szilagyi, A., Banoczy, Z., Hudecz, F., and Friedrich, P. (2004) *J. Biol. Chem.* **279**, 20775–20785
56. Choe, Y., Leonetti, F., Greenbaum, D. C., Lecaille, F., Bogyo, M., Bromme, D., Ellman, J. A., and Craik, C. S. (2006) *J. Biol. Chem.* **281**, 12824–12832
57. Lee, T. W., Cherney, M. M., Huitema, C., Liu, J., James, K. E., Powers, J. C., Eltis, L. D., and James, M. N. (2005) *J. Mol. Biol.* **353**, 1137–1151
58. Schaschke, N., Assfalg-Machleidt, I., Machleidt, W., Turk, D., and Moroder, L. (1997) *Bioorg. Med. Chem.* **5**, 1789–1797